metals

MDPI

Article

Pre-Aging Effect on the Formation of Ω Phase and Mechanical Properties of the Al-Cu-Mg-Ag Alloy

Puyou Ying [1], Changhong Lin [1,*], Zhiyi Liu [2,*], Song Bai [2], Vladimir Levchenko [1], Ping Zhang [1], Jianbo Wu [1], Tao Yang [1], Min Huang [1], Gang Yang [3], Meng Liu [4] and Mengjia Li [5]

1 Zhejiang Provincial Key Laboratory for Cutting Tools, Taizhou University, Jiaojiang 318000, China; ypu@tzc.edu.cn (P.Y.); vladalev@yahoo.com (V.L.); zhangp03@tzc.edu.cn (P.Z.); wujb@tzc.edu.cn (J.W.); yangtaochd@163.com (T.Y.); mhuang@tzc.edu.cn (M.H.)
2 School of Material Science and Engineering, Central South University, Changsha 410083, China; baisongmse@csu.edu.cn
3 School of Mechatronics and Mold Engineering, Taizhou Vocational College of Science & Technology, Taizhou 318000, China; gangyang@tzvcst.edu.cn
4 College of Materials and Chemical Engineering, Pingxiang University, Pingxiang 337055, China; liumeng6960@163.com
5 School of Materials Science and Engineering, Zhengzhou University, Zhengzhou 450001, China; mengjia.li@zzu.edu.cn
* Correspondence: lin201191@163.com (C.L.); liuzhiyi@csu.edu.cn (Z.L.)

Abstract: In the present work, different aging treatments were performed to investigate the pre-aging effect on the formation of Ω phase and mechanical properties in Al-Cu-Mg-Ag alloy. The results showed that pre-strain could inhibit the formation of Ω phases, which was detrimental to the alloy strength. Due to the introduction of pre-aging treatment before pre-strain, the adverse effect of pre-strain on the precipitation of the Ω phase was reduced, and the alloy strength was increased by at least 15 MPa. Besides this, increasing the pre-aging temperature promoted the precipitation of Ω phases, inhibited the formation of θ′ phases, and improved the alloy strength. This was because the higher pre-aging temperature promoted more pre-precipitated Ω phases in the pre-aging process, and most of the pre-precipitated Ω phases could be retained and grew in the subsequent aging process. As a result, the tensile strength of the alloy increased from 523 MPa to 540 MPa. In addition, pre-aging with a higher temperature consumed more solute atoms, leading to less residual solute atoms in the matrix. Thus, the adverse effects of pre-strain, which inhibit the formation of clusters by the segregation of solute atoms, were reduced.

Keywords: pre-aging; Ω phase; Al-Cu-Mg-Ag alloy; pre-strain; pre-aging temperature; mechanical property

check for updates

Citation: Ying, P.; Lin, C.; Liu, Z.; Bai, S.; Levchenko, V.; Zhang, P.; Wu, J.; Yang, T.; Huang, M.; Yang, G.; et al. Pre-Aging Effect on the Formation of Ω Phase and Mechanical Properties of the Al-Cu-Mg-Ag Alloy. *Metals* **2022**, *12*, 1208. https://doi.org/10.3390/met12071208

Academic Editor: Sergey Konovalov

Received: 23 June 2022
Accepted: 15 July 2022
Published: 16 July 2022

1. Introduction

As a heat-resistant aluminum alloy, the Al-Cu-Mg-Ag alloy is superior to conventional alloys, such as 2124, 2219, and 2618 alloys [1–3]. Adding Ag to the Al-Cu-Mg alloy forms hexagonal-shaped disk-like precipitations on the primary slip plane $\{111\}_a$ of the matrix, known as the Ω phase [4–7]. The Ω phase, with a high aspect ratio, is responsible for the excellent mechanical properties of the Al-Cu-Mg-Ag alloy [4,8]. Therefore, Al-Cu-Mg-Ag alloy can meet the high temperature requirement of aircraft structural parts for aerospace applications.

The main strengthening precipitations of Al-Cu-Mg-Ag alloy are the Ω and θ′ phases, and the strengthening effect of the Ω phase is superior to that of the θ′ phase [9]. According to the works done in Refs. [6,10], the precipitation sequence in the Al-Cu-Mg-Ag alloy is summarized as follows: α_{sss}→GP zone→θ′′→θ′→θ (Al_2Cu) and α_{sss}→Mg-Ag co-cluster→Ω→θ. There is a competitive precipitation relationship between the Ω phase and θ′ phase, and the competitive precipitation kinetics are affected by several aspects:

alloy composition (e.g., the Ag content [11–15]), pre-strain process [16–20] and the aging treatment [20–22].

Extensive research works [11–14] have shown that a high Ag content is favorable for forming the Mg-Ag cluster, which is the precursor of the Ω phase. The increase in the Ag content facilitates the nucleation and precipitation of the Ω phase. Thus, a high Ag content can improve the strength of the Al-Cu-Mg-Ag alloy. Based on the above results, the Al-Cu-Mg-Ag alloy with a high Ag content was selected to carry out relevant research in this work.

A pre-strain is usually applied in the as-quenched state to relieve quench-induced residual stress [16–20,23–25]. It is widely recognized that the presence of dislocations produced by pre-strain greatly affects the precipitation behavior and mechanical properties of the Al-Cu-Mg-Ag alloy [16–20,24–30]. A study by Ringer et al. [16] suggested the aging hardening response of the Al-Cu-Mg-Ag alloy was reduced by cold work. This was because the number density of Ω plates was reduced, while the density of θ′ plates was increased, due to the presence of dislocations. Li and Shenoy [17] also found that pre-strain prior to aging resulted in a drastic reduction of Ω volume fraction and a simultaneous enhancement of θ′ precipitation, in agreement with Refs. [18–20]. Chen et al. [18] claimed the passage of dislocations through the α-matrix disrupted the Mg-Ag clustering, and dislocations were the sites for the heterogeneous nucleation of θ′ phase. Bai et al. [19,20] reported that deformation before artificial aging suppressed Mg-Ag co-clustering, leading to a decrease in the number density of Ω plates and an increase in the number density of θ′ phases. Gazizov and Kaibyshev [25,26] proposed that intense plastic deformation contributed to the transformation from Ω phase to θ phase. Thus, in the mentioned studies, the alloy strength decreased due to the introduction of the pre-strain, which decreased the number density of Ω phase [16–20,25,26]. Ünlü et al. [24] found that a 6% pre-strain level improved the mechanical properties of the Al-Cu-Mg ternary alloy by increasing the number density of Ω and θ′ phases, as well as refining the size of precipitates. However, the number density of Ω phase in the Al-Cu-Mg ternary alloy was much lower than that of Ag-containing alloy, indicating that the mechanical properties of the Ag-free alloy were far inferior to those of the Ag-containing alloy. Liu et al. [25] reported that with increase in the pre-strain level, the alloy strength decreased first and then increased. The sample with a 6% pre-strain possessed the highest tensile strength, due to the refined precipitates. Gazizov and Kaibyshev [26] found that an increased peak hardness was achieved with increasing cold rolling strain because cold rolling induced the formation of deformation bands. Therefore, introducing large deformation before aging can bring in deformation bands or refine precipitate size, thus improving the mechanical properties of the Al-Cu-Mg-Ag alloy [25,26].

However, until the present time, only a few reports have proposed methods to enhance the mechanical properties of pre-deformed Al-Cu-Mg-Ag alloy. One effective approach of enhancing the mechanical properties of aluminum alloy is to adopt severe plastic deformation (SPD) techniques. SPD techniques are applicable processes for producing ultrafine grained structures by introducing large deformation. In the works done by Refs. [27–30], the mechanical properties of aluminum alloy could be improved by equal-channel angular pressing (ECAP) and multi-directional forging (MDF) techniques. However, this is not practical in commercial practice, especially for the production of aluminum alloy sheet where a small pre-strain (~3%) is applied. Aging treatment optimizations, such as interrupted aging, can effectively improve the mechanical properties of the Al-Cu-Mg-Ag alloy. However, interrupted aging treatment (e.g., T6I6 treatment in Ref. [21]) costs too much in time during lower-temperature aging in the Al-Cu-Mg-Ag alloy [21], so is not practical either. In our previous work [22], a type of duplex aging was invented, aimed at achieving more Ω precipitates by controlling the competitive precipitation between Ω and θ′ phases, and thus, increasing the strength of the pre-strained Al-Cu-Mg-Ag alloy. The present work aimed to develop a new aging treatment to assist the precipitation of the Ω phase and reduce the unfavorable effect of pre-strain on the mechanical properties of the Al-Cu-Mg-Ag alloy with a high Ag content.

2. Materials and Methods

In this study, an Al-Cu-Mg-Ag hot rolling sheet (2.6 mm thick) was used. The chemical composition of the studied alloy is listed in Table 1. The sheet was solution-treated at 520 °C for 2 h, water quenched, and immediately aged under different conditions. The detailed heat treatments are shown in Table 2. Temper-0 was the usual heat treatment of the T8 process, in which it was pre-stretched by 2.5% and aged at 165 °C for 16 h to peak age. Temper-7, temper-8, and temper-9 were the proposed aging treatments to reduce the unfavorable effects of pre-strain, which were treated as pre-aging + 2.5% pre-stretch + secondary aging to peak age. To clarify the effect of each heat treatment step on the microstructure and properties of the alloy, temper-1 ~ temper-6 were applied. Temper-1, temper-2, and temper-3 were the pre-aging steps in the treatment process, which were 165 °C/1 h, 180 °C/1 h, and 190 °C/1 h, respectively. Temper-4, temper-5, and temper-6 were treated with pre-stretch after corresponding pre-aging, which were 165 °C/1 h + 2.5% pre-stretch, 180 °C/1 h + 2.5% pre-stretch, and 190 °C/1 h + 2.5% pre-stretch, respectively.

Table 1. Chemical composition of the studied alloy (wt. %).

Element	Cu	Mg	Ag	Mn	Ti	Zr	Al
	6.5	0.4	1.6	0.3	0.05	0.10	Bal.

Table 2. Description of heat treatments for the studied alloy.

Temper	Solution Treatment	Pre-Aging	Pre-Strain	Secondary Aging
Temper-0	520 °C/2 h	None	2.5%	165 °C/16 h
Temper-1	520 °C/2 h	165 °C/1 h	None	None
Temper-2	520 °C/2 h	180 °C/1 h	None	None
Temper-3	520 °C/2 h	190 °C/1 h	None	None
Temper-4	520 °C/2 h	165 °C/1 h	2.5%	None
Temper-5	520 °C/2 h	180 °C/1 h	2.5%	None
Temper-6	520 °C/2 h	190 °C/1 h	2.5%	None
Temper-7	520 °C/2 h	165 °C/1 h	2.5%	165 °C/16 h
Temper-8	520 °C/2 h	180 °C/1 h	2.5%	165 °C/12 h
Temper-9	520 °C/2 h	190 °C/1 h	2.5%	165 °C/6 h

Specimens for tensile testing were prepared vertical to the rolling direction of the sheets. Tensile testing of all specimens was conducted on an electronic universal testing machine (SANS-CMJ5105, MTS Systems (China) Co., Ltd., Shenzhen, China) at ambient temperature with a 2 mm/min loading speed. The mechanical properties in the present work were the average values of three samples for each tested condition.

Samples used for transmission electron microscopy (TEM, Tecnai-G^2 20, FEI, Hillsboro, OR, USA) observation were thin disks of 3 mm diameter, which were twin-jet electropolished in a 70% ethanol and 30% nitric acid solution at −25 °C. These were then examined by TEM at accelerating voltage of 200 kV.

Quantitative analysis of the number density and particle size of Ω plates was performed using Nano Measurer software (Version 1.2.5, Fudan University, Shanghai, China). The truncation effects of the plate-like precipitates were eliminated by a stereological correction method [31]. In the present work, the average values were reported for the number density and particle size of the Ω phase. A minimum of 4 TEM images were chosen to determine the number density of Ω phase, and a minimum of 500 Ω plates were measured to determine the average particle size, to reduce statistical errors.

3. Results

3.1. Mechanical Properties of Samples with Different Heat Treatments

The results of the tensile tests of the samples with different pre-aging treatments (temper-1, temper-2, and temper-3) are presented in Table 3. With increasing temperature of pre-aging from 165 °C to 180 °C, both yielded strength and tensile strength increased, while elongation decreased from 23.4% to 9.1%. When the temperature of pre-aging further increased to 190 °C, yield strength and tensile strength further increased as well, while elongation decreased to 8.3%. When a pre-strain was applied after pre-aging (temper-4, temper-5, and temper-6), the alloy strength decreased. In addition, when the temperature of pre-aging before pre-strain increased from 165 °C to 190 °C, the alloy strength enhanced, while elongation dropped.

Table 3. Tensile properties of the Al-Cu-Mg-Ag alloy with different treating tempers at room temperature.

Tempers	Tensile Strength σ_b/MPa	Yield Strength $\sigma_{0.2}$/MPa	Elongation (%)
Temper-0	508 ± 5	482 ± 5	8.6 ± 0.1
Temper-1	429 ± 4	281 ± 7	23.4 ± 2.5
Temper-2	502 ± 3	470 ± 4	9.1 ± 0.2
Temper-3	527 ± 3	502 ± 1	8.3 ± 0.3
Temper-4	416 ± 6	277 ± 5	24.0 ± 1.8
Temper-5	495 ± 4	468 ± 3	9.3 ± 0.3
Temper-6	524 ± 4	502 ± 2	8.3 ± 0.2
Temper-7	523 ± 1	500 ± 1	8.1 ± 0.1
Temper-8	533 ± 3	501 ± 5	7.2 ± 0.3
Temper-9	540 ± 1	506 ± 4	6.8 ± 0.1

The tensile testing results of samples treated with secondary aging to peak age (temper-0, temper-7, temper-8, and temper-9) are also given in Table 3. Compared to temper-0, temper-7 was treated with a pre-aging of 165 °C/1 h, possessing higher strength and similar elongation. This indicated that when a pre-aging of 165 °C/1 h was applied, temper-7 possessed better tensile property than temper-1. When a pre-aging of 180 °C/1 h was applied, temper-8 possessed higher strength and lower elongation, compared to temper-0 and temper-7. Moreover, temper-9 possessed the highest yield strength, tensile strength, and the lowest elongation of the four tempers. It can be seen that when pre-aging was applied, the yield strength and tensile strength increased. Furthermore, when the temperature of pre-aging increased, the yield strength and tensile strength could be further increased.

3.2. TEM Characterization for Different Heat Treatments

Typical microstructures of the studied alloys aged with different treating tempers (as mentioned in Table 2) were characterized by the TEM technique. In addition, the corresponding selected area electron diffraction (SAED) patterns are also demonstrated in the related figures. The diffraction spots at 1/3, 2/3 $\{220\}_\alpha$ and the streaks along $<111>_\alpha$ directions were produced by Ω phases. The diffraction spot at 1/2 $\{220\}_\alpha$ position and the streaks along $<100>_\alpha$ directions were induced by θ′ phases. Generally, the intensity of diffraction spots and streaks in the SAED patterns could roughly reflect the volume fraction of precipitates. Quantitative TEM analysis of the microstructures were performed to carry out the average number density and relative frequency of corresponding Ω plates in the related alloys.

3.2.1. TEM Characterization of the Studied Alloys after the Pre-Aging Process

Figure 1a–c shows the microstructures of the studied alloys after the pre-aging process (temper-1, temper-2, and temper-3). As seen in Figure 1a–c, when the pre-aging of 165 °C/1 h was applied, the number density of θ′ precipitation in Figure 1a was the highest, compared with those in Figure 1b,c, in which a high-temperature pre-aging was applied. It can also be confirmed by the streaks along $<100>_\alpha$ directions and the weak intensity of the spots at 1/2 $\{220\}_\alpha$ positions in Figure 1a. When the pre-aging temperature increased to 180 °C, a small quantity of θ′ phase was observed in Figure 1b. In Figure 1c, only a few θ′ can be seen. A high density of Ω plates was seen in Figure 1a–c, in agreement with the clear diffraction spots at 1/3 and 2/3{220}$_\alpha$ positions. Moreover, the number density of Ω plates increased as the temperature of pre-aging increased from 160 °C to 190 °C. Therefore, it can be inferred that when the alloy was treated with pre-aging for 1 h, a higher aging temperature was favorable for the precipitation of the Ω phase, while the precipitation of the θ′ phase was restrained.

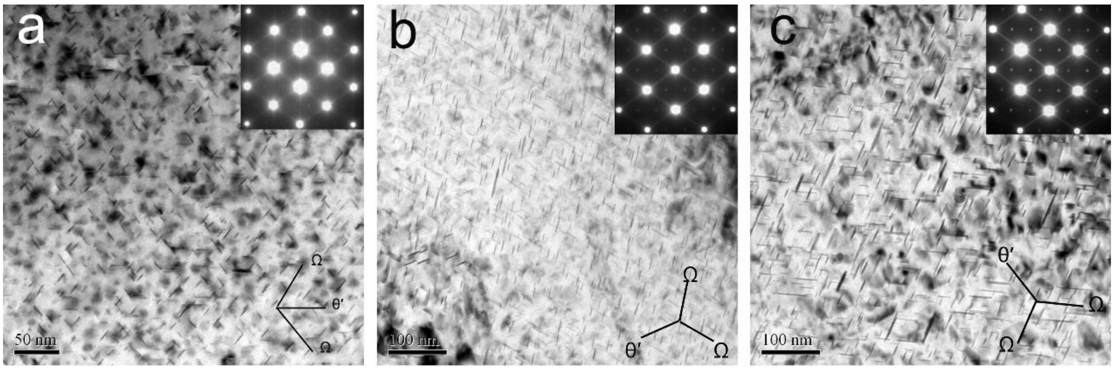

Figure 1. Bright field TEM images showing the microstructures of the studied alloys after the pre-aging process: (**a**) temper-1, (**b**) temper-2, and (**c**) temper-3. All the images were taken near (110)$_\alpha$ orientations.

Figure 2 provides the average number density and relative frequency of various Ω plates in the studied alloys after the pre-aging process. It was found that the Ω precipitations were mainly composed of plates with a diameter from 0 to 20 nm, and large Ω plates with a diameter larger than 20 nm were not detected in temper-1. Obviously, when the temperature of pre-aging increased, the size of the Ω precipitations grew, as large Ω plates with a diameter from 20 nm to 50 nm appeared in temper-2 and temper-3. That is to say, compared to temper-1, pre-aging with a high temperature facilitated the precipitation of Ω plates with a larger diameter, ranging from 20 to 50 nm, as shown in Figure 2.

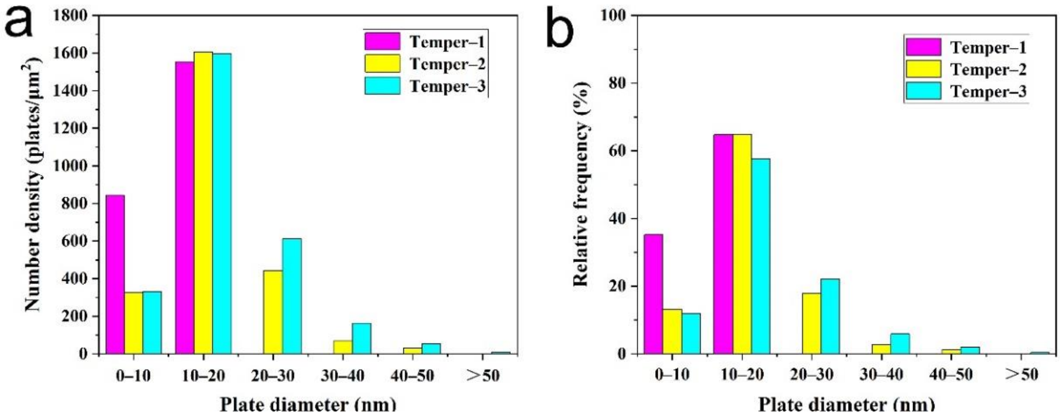

Figure 2. Plots of (**a**) the average number density and (**b**) the relative frequency of various Ω plates in the studied alloys after the pre-aging process.

3.2.2. TEM Characterization of the Studied Alloys Treated with Pre-Strain after Pre-Aging

The microstructures of samples treated with pre-strain after pre-aging are exhibited in Figure 3a–c. As shown in Figure 3a,b, with a pre-strain applied after pre-aging at 165 °C and 180 °C, a noticeable increase in the number density of θ′ precipitation can be seen, as compared to Figure 1a,b. However, in Figure 3c, only a few θ′ could be seen, which is similar to Figure 1c. The number density of θ′ precipitation in Figure 3a was higher than those in Figure 3b,c, which could be confirmed by the corresponding SAED patterns, as streaks along <111>$_\alpha$ directions were only detected in Figure 3a. In Figure 3a–c, Ω-dominated microstructures can be seen and the number density of Ω plates increased as the temperature of pre-aging increased from 160 °C to 190 °C. Moreover, what is interesting is that when a pre-strain was applied, the number density of Ω plates decreased. Furthermore, when the aging temperature increased, whether the pre-strain was applied or not, the plate diameter of Ω phase increased. In summary, when a pre-strain was applied after the pre-aging, the number density of the θ′ phase increased, while the number density of Ω phase decreased. When the studied alloys were treated with pre-strain after pre-aging, a higher pre-aging temperature contributed to the precipitation of the Ω phase while the precipitation of the θ′ phase was suppressed.

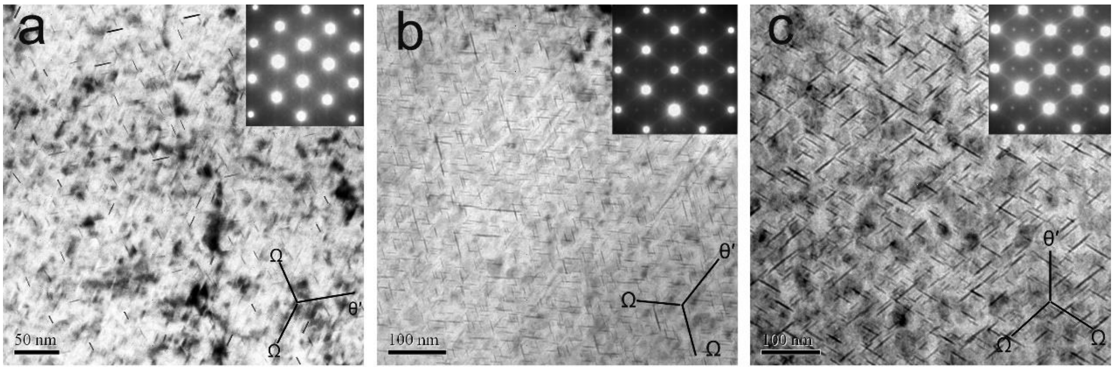

Figure 3. Bright field TEM images showing the microstructures of samples treated with pre-strain after pre-aging: (**a**) temper-4, (**b**) temper-5, and (**c**) temper-6. All the images were taken near $(110)_\alpha$ orientations.

The average number density and relative frequency of various Ω plates of tempers 4–6 is displayed in Figure 4. The Ω precipitations were mainly composed of plates with a diameter ranging from 0 to 20 nm in temper-4, similar to temper-1. It was obvious that when the temperature of the pre-aging increased, the number density of the Ω precipitations increased and the size of the Ω precipitations grew, again confirming that a higher pre-aging temperature was beneficial to the precipitation of Ω phase.

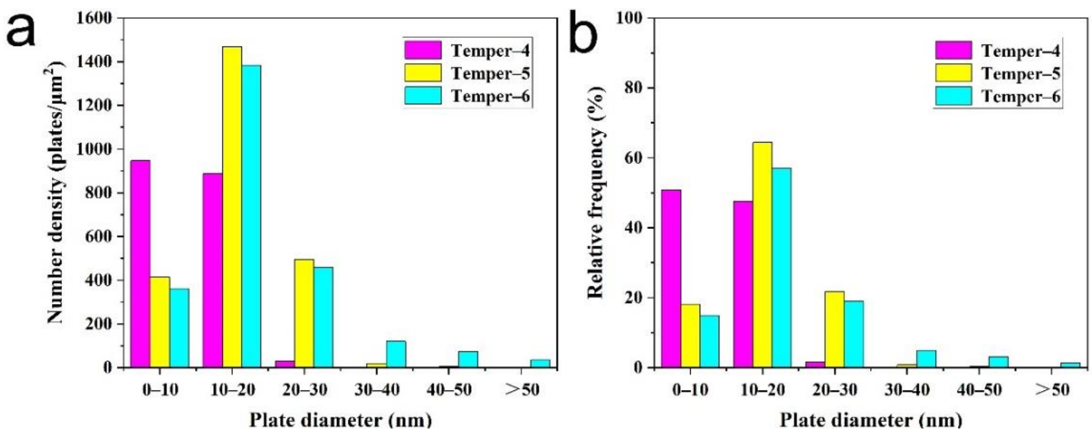

Figure 4. Plots of (**a**) the average number density and (**b**) the relative frequency of various Ω plates in the studied alloys treated with pre-strain after pre-aging.

3.2.3. TEM Characterization of the Studied Alloys Treated with the Final Heat Treatment Process

Typical microstructures of the studied alloys treated with the final heat treatment process (temper-0, temper-7, temper-8, and temper-9) are demonstrated in Figure 5a–d. As shown in Figure 5a, the number density of θ′ was obviously higher than those of other tempers. Meanwhile, the number density of Ω plates was the lowest in temper-0. When a pre-aging of 165 °C/1 h was applied, the number density of θ′ decreased, as shown in Figure 5b, which could be confirmed by the weaker intensity of the spots at 1/2 $\{220\}_\alpha$ positions. When high-temperature pre-aging was adopted, as seen in Figure 5c,d, only a few θ′ could be seen. Corresponding SAED patterns supported this, as no spots at 1/2$\{220\}_\alpha$ positions were detected. The number density of Ω plates increased in Figure 5b,d as compared to that in Figure 5a. Besides, compared to temper-7 with the pre-aging of 165 °C, the number density of Ω plates increased as the temperature of pre-aging increased to 180 °C in temper-8 and 190 °C in temper-9. Again, this indicated that a high temperature of pre-aging suppressed the formation of θ′ phase and facilitated the formation of Ω phase, which is consistent with the results in Figures 1 and 3.

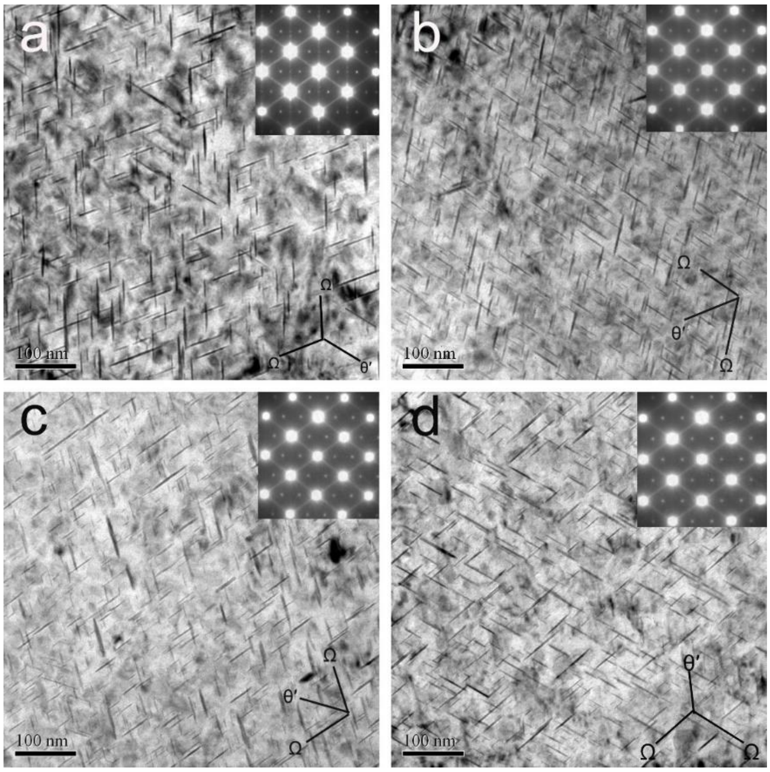

Figure 5. Bright field TEM images showing the microstructures of samples aged with the final heat treatment process: (**a**) temper-0, (**b**) temper-7, (**c**) temper-8, and (**d**) temper-9. All the images were taken near $(110)_\alpha$ orientations.

Compared to temper-0, samples treated with pre-aging (temper-7, temper-8 and temper-9) facilitated the precipitation of Ω plates as the number density of Ω plates was higher in temper-7, temper-8, and temper-9, as shown in Figure 6. Moreover, when the higher temperature of pre-aging was applied, the number density of Ω phase was higher. In Figure 6b, the relative frequency of Ω plates with a diameter below 20 nm in temper-0 was lower than those in tempers 7–9, while the relative frequency of Ω plates with a diameter above 20 nm showed the opposite trend. This indicated that pre-aging could refine the Ω phase size. Besides, the relative frequency of Ω plates with a diameter below 20 nm in temper-7 was higher than those in temper-8 and temper-9, while the relative frequency of Ω plates with a diameter above 20 nm showed the opposite trend. This indicated that pre-aging with a high temperature increased the Ω phase size.

3.3. Quantitative TEM Results of Ω Plates for Different Heat Treatments

Corresponding quantitative TEM results of Ω plates for different heat treatments are given in Table 4. As seen in Table 4, the number density of Ω plates in samples with different pre-aging treatments (temper-1, temper-2, and temper-3) increased as the pre-aging temperature increased from 160 °C (2396 plates/μm^2) to 180 °C (2475 plates/μm^2) and 190 °C (2765 plates/μm^2). Further, the plate diameter of Ω plates increased as the pre-aging temperature increased from 160 °C (11.0 nm) to 180 °C (16.4 nm) and 190 °C (17.9 nm).

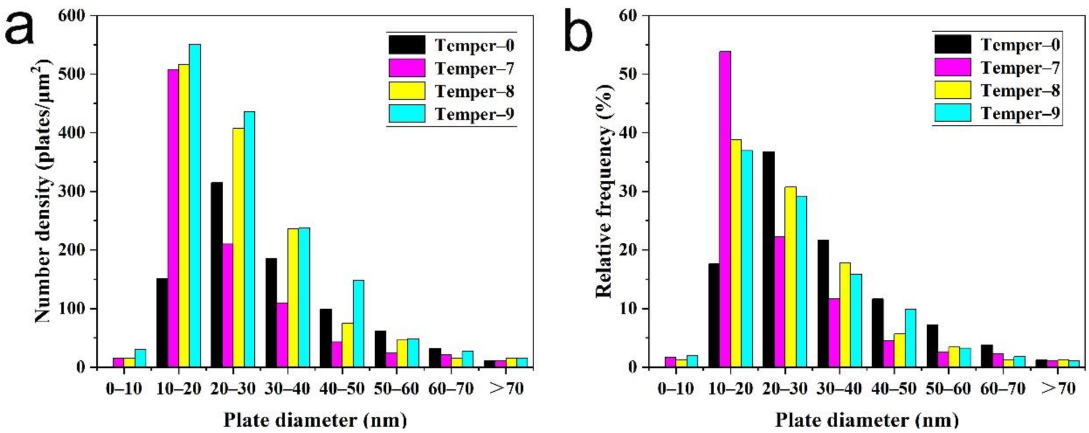

Figure 6. Plots of (**a**) the average number density and (**b**) the relative frequency of various Ω plates in the studied alloys treated with the final heat treatment process.

Table 4. Summary of quantitative TEM results of Ω plates in samples with different aging treatments.

Aging Treatments	Average Plate Diameter (nm)	Number Density (Plates/μm^2)
Temper-1	11.0	2396
Temper-2	16.4	2475
Temper-3	17.9	2765
Temper-4	10.7	1863
Temper-5	15.7	2275
Temper-6	17.8	2430
Temper-0	32.2	854
Temple-7	23.7	943
Temper-8	26.0	1330
Temper-9	26.5	1492

When the samples were treated with pre-strain after pre-aging (temper-4, temper-5, and temper-6), the number density of Ω plates also increased as the temperature of pre-aging increased from 160 °C (1863 plates/μm^2) to 180 °C (2275 plates/μm^2) and 190 °C (2430 plates/μm^2). When the pre-strain was applied after pre-aging at 165 °C, 180 °C, and 190 °C, the number density of Ω plates decreased from 2396 plates/μm^2, 2475 plates/μm^2, and 2765 plates/μm^2 to 1863 plates/μm^2, 2275 plates/μm^2, and 2430 plates/μm^2, respectively. Furthermore, when the aging temperature increased, the plate diameter increased. However, when the pre-strain was applied after pre-aging, the plate diameter was similar.

Quantitative TEM results of Ω plates in the samples treated with the final heat treatment process (temper-0, temper-7, temper-8, and temper-9) are also presented in Table 4. When a pre-aging of 165 °C/1 h was applied, the number density of Ω plates increased from 854 plates/μm^2 to 943 plates/μm^2. When the temperature of pre-aging increased to 180 and 190 °C, the number density of Ω plates further increased to 1330 plates/μm^2 and 1492 plates/μm^2, respectively. Further, the plate diameter of Ω plates decreased from 32.2 nm in temper-0 to 23.7 nm in temper-7, then increased to 26.0 and 26.5 nm in temper-8 and temper-9, respectively. This indicated that, compared with temper-0, the Ω phase size was refined by pre-aging and the size increased with the pre-aging temperature. In addition, it can be seen from Table 4 that when secondary aging was applied (temper-7, temper-8, and temper-9) after pre-aging and pre-strain (temper-4, temper-5, and temper-6), the Ω plate diameter increased, while the number density of Ω plates decreased.

4. Discussion

The competitive precipitation kinetics between Ω and θ′ precipitates in the Al-Cu-Mg-Ag alloy is influenced by several factors: (e.g., the Ag content [11–15], pre-strain process [16–20] and aging treatment [20–22]). For a given Al-Cu-Mg-Ag alloy with a high Ag content, since pre-strain is applied in the as-quenched state to relieve residual stress, the following aging process needs to adjust to modify the precipitation behavior between Ω and θ′ precipitates.

4.1. The Effect of Pre-Strain on the Precipitation Behavior of the Studied Alloy

Comparing the number density of Ω phase in temper-1 and temper-4, temper-2 and temper-5, temper-3 and temper-6, it clearly indicated that when a pre-strain was applied, the number density of Ω plates decreased, as shown in Table 4. That is to say, the formation of Ω phase was inhibited as the pre-strain was applied. This was because the concentration of vacancies and Cu atoms in the matrix was changed by the dislocations which were introduced by the pre-strain.

After solid-solution and water quenching, Cu, Mg, and Ag solute atoms in the matrix were in a supersaturated state. At the same time, due to the rapid cooling of quenching, a large number of vacancies were retained in the matrix. Therefore, when the alloy was artificially aged after quenching, the high concentration of solute atoms could form clusters in the matrix. The diffusion of solute atoms to form clusters depended on vacancy, so the vacancy concentration in the matrix determined the nucleation of clusters. This was because solute atoms could be combined with vacancies to form solute-vacancy clustering (such as Mg/Ag/vacancy clustering and Cu/Mg/vacancy clustering), which could minimize the elastic strain energy [32–34]. Generally, due to the strong interaction between the vacancy and Mg and Ag atoms, the formation of Mg-Ag clusters at the beginning of aging was promoted in the Al-Cu-Mg-Ag alloy [20]. However, when pre-strain was applied, the number density of dislocation increased, leading to the loss of vacancies [16,18–20]. Ringer [16] found that the response of Al-Cu-Mg, Al-Cu-Mg-Ag and Al-Cu-Li-Mg-Ag alloys to hardening during natural aging were reduced by pre-strain. This phenomenon arose because the vacancy would be annihilated at dislocation lines and tangles. Work done by Chen [18] pointed out that the formation rates of Al-Cu and Mg-Ag clustering were restrained by dislocations, which acted as sinks for vacancies. Bai's results [19,20] by APT analysis proved that Mg-Ag co-clusters were restrained by pre-strain. It was due to the annihilation of vacancies at dislocation lines and tangles because excessive vacancies tended to eliminate at dislocations. Combined with the above research results, it can be inferred that the concentration of vacancies reduced as pre-strain was applied. The loss of vacancies inhibited the formation of Mg-Ag clustering.

In addition, extensive research work has proposed that dislocations were the heterogeneous nucleation sites for θ′ phase [15–20]. That is to say, dislocations introduced by pre-strain favored the precipitation of θ′ phase. This can be found in Figure 3 of tempers 4–6, where the number density of θ′ phase increased after the pre-strain was applied. The nucleation and precipitation process of θ′ phase consumed Cu atoms, which were also required by the formation of Ω phases. Ringer pointed out that Mg-Ag clusters grew into MgCuAg complexes with the involvement of Cu atoms, and then formed Ω phases [6]. Thus, the formation of Ω phase was inhibited due to the lack of Cu atoms, which were consumed by forming the θ′ phases. The decrease in the number density of Ω phase in Figure 3 and Table 4 of tempers 4–6 supported this opinion. It is consistent with the results in Refs. [19,20]. Therefore, pre-strain favored the precipitation of θ′ phase and consumed Cu atoms, leading to a decrease in the number density of Ω phase.

In conclusion, pre-strain inhibited the clustering of Mg-Ag atoms, because the dislocation reduced the concentration of vacancies. In addition, the dislocations promoted the precipitation of θ′ phase and consumed Cu atoms. The combination of these two factors meant the formation of Ω phases was inhibited as pre-strain was applied.

4.2. The Effect of Pre-Aging on the Precipitation Behavior and Mechanical Properties of the Studied Alloy

Comparing the number density of Ω phase in temper-7, temper-8, and temper-9 with that in temper-0, it evidently showed that when pre-aging was applied, the number density of Ω plates increased while the number density of θ′ phases decreased, as shown in Figure 5 and Table 4. In the meantime, when pre-aging was applied, the yield strength and tensile strength increased, as given in Table 3. That is to say, introducing the pre-aging process promoted the precipitation of Ω phases, inhibited the formation of θ′ phases, and improved the alloy strength.

The alloys after pre-aging treatment (temper-1, temper-2, temper-3) were still in an under-aged state. As shown in Figure 1, Ω and θ′ phases were formed after pre-aging. In addition to Ω and θ′ phases, Mg-Ag clusters, Cu-Mg clusters, G.P. zones, and the remaining solute atoms also existed in the matrix [20]. Though the subsequent pre-strain process inhibited the clustering of Mg-Ag atoms and the formation of Ω phases, as mentioned in Section 4.1, the pre-precipitated Ω phases still existed in the matrix and grew during the following secondary aging process, thus reducing the adverse effect of pre-deformation on the precipitation of Ω phase. As a result, the number density of Ω phase in temper-7, temper-8, and temper-9 was more than that in temper-0, while the number density of θ′ phase in temper-0 was more than those in temper-7, temper-8, and temper-9. As the contribution of Ω relative to the alloy strength was stronger than that of θ′ phase [35–37], the tensile properties of the alloy treated with temper-7, temper-8, and temper-9 were better than the alloy treated with temper-0.

In conclusion, due to the introduction of the pre-aging treatment before pre-deformation, most of the precipitated Ω phase could be retained and grew in the subsequent aging process, thus reducing the adverse effect of pre-deformation on the precipitation of Ω phase.

4.3. The Effect of the Pre-Aging Temperature on the Precipitation Behavior and Mechanical Properties of the Studied Alloy

Comparing the number density of Ω phase in temper-7, temper-8, and temper-9, it was evident that when the pre-aging temperature was increased, the number density of Ω plates increased, while the number density of θ′ phases decreased, as shown in Figures 5 and 6, and Table 4. In the meantime, when the pre-aging temperature was increased, the yield strength and tensile strength increased, as shown in Table 3. That is to say, increasing the pre-aging temperature promoted the precipitation of Ω phases, inhibited the formation of θ′ phases and improved the alloy strength.

According to the analysis in Section 4.2, the pre-aging treatment before pre-deformation was favorable for the precipitation of Ω phase and the alloy strength due to the pre-precipitated Ω phase. Therefore, one effect of the pre-aging temperature was that it determined the number density of the precipitated Ω phase during the pre-aging process. From Figure 1, it is obvious that a higher aging temperature was favorable for the precipitation of Ω phase while the precipitation of θ′ phase was restrained. This could be explained by the following four aspects.

First of all, it is well known that vacancy concentration is related to temperature, and the vacancy concentration increased with temperature increase. Since Mg-Ag clusters were formed by combining Mg and Ag atoms with vacancies [6,38], the increase in the vacancy concentration was favorable for the formation of Mg-Ag clusters. Thus, the increase in aging temperature was conducive to the formation of Mg-Ag clusters, which could provide more nucleation sites for Ω phase. Second, the nucleation of Ω phase was a diffusion process in which supersaturated solute atoms combined with vacancies. Obviously, increasing the aging temperature could accelerate the diffusion of solute atoms and vacancies, which was more conducive to the nucleation of Ω phase. Third, there was a large mismatch between the Ω phase and the matrix in the direction perpendicular to $\{111\}_{Al}$ [39], resulting in a large phase transition resistance. Increasing the temperature could increase the driving force for the phase transformation and facilitate Ω phase precipitation from the matrix. Fourth, the formation of Ω phase required the diffusion of Cu atoms into Mg-Ag clusters [4,40,41]. Increasing the temperature could promote the migration rate of Cu atoms, which was also conducive to improving the nucleation rate of Ω phases.

All the factors mentioned above indicate that increasing the pre-aging temperature would promote the precipitation of Ω phase and increase the number density of precipitated Ω phases. The precipitation of Ω phase consumed a large number of Cu atoms in the matrix, inhibiting the precipitation of θ′ phase. This is consistent with the results of TEM observation in Figure 1 and quantitative analysis in Figure 2 and Table 4. Though the alloy is still in an under-aged state after pre-aging treatment, a higher temperature of pre-aging could make the aging more sufficient. As a result, the size of precipitated Ω phase increased with increasing aging temperature, consistent with the results in Figure 2 and Table 4.

After pre-aging, pre-strain was applied, resulting in a decrease in the number density of Ω phase. However, the number density of Ω phase in the deformed alloy still increased with increase in the pre-aging temperature. This was mainly because most of the Ω phases precipitated by pre-aging could be retained, and the number density of Ω phase was higher in the alloy treated with a higher pre-aging temperature. Finally, secondary aging was applied to peak aging, and the remaining Ω phase grew, so the number of Ω phases in the alloy increased with increase in the pre-aging temperature.

In addition, the alloys were still in an under-aged state after pre-aging treatment (temper-1, temper-2, temper-3). However, with a higher pre-aging temperature, alloy aging was more sufficient, and the number density of clusters and Ω phases was higher. The formation of these clusters and the growth of the phase consumed solute atoms in the matrix. Obviously, the higher aging temperature consumed more solute atoms, so the residual solute atoms in the matrix became less. Since pre-deformation inhibited the formation of clusters by affecting the segregation of solute atoms, the residual solute atoms in the matrix with a high pre-aging temperature were less, so the adverse effects of pre-deformation were reduced. Conversely, the alloy with a low pre-treatment temperature (especially 165 °C/1 h) had more solute atoms in the matrix, which was more adversely affected by pre-deformation.

In conclusion, increasing the pre-aging temperature promoted the precipitation of Ω phases, inhibited the formation of θ′ phases, and improved alloy strength. This was due to the higher pre-aging temperature promoting a more precipitated Ω phase in the pre-aging process, and most of the precipitated Ω phase could be retained and grew in the subsequent aging process. In addition, pre-aging with a higher temperature consumed more solute atoms, leading to less residual solute atoms in the matrix. These two factors contributed to reducing the adverse effect of pre-deformation on the precipitation of Ω phase.

5. Conclusions

The pre-aging effect on the Ω phase formation and mechanical properties of the Al-Cu-Mg-Ag alloy was investigated in this work. The results are summarized below.

(1) Pre-strain decreased alloy strength. This negative effect could be reduced by introducing pre-aging treatment. Furthermore, pre-aging with a higher temperature was more beneficial to alloy strength.

(2) Pre-strain inhibited the formation of Ω phases. When pre-aging was applied, the pre-precipitated Ω phase could be retained and grew in the subsequent aging process. This reduced the adverse effect of pre-strain.

(3) A higher pre-aging temperature could promote more pre-precipitated Ω phase, finally increasing the number density of Ω phases in the matrix. Moreover, the precipitated Ω phase consumed solute atoms, which indicated that a higher pre-aging temperature could expend more solute atoms and less residual solute atoms remained in the matrix. Thus, the formation of clusters by the segregation of solute atoms were less affected by pre-strain.

Author Contributions: P.Y., investigation, formal analysis, writing—original draft preparation; C.L., writing—review and editing, data curation; Z.L., conceptualization, methodology, funding; S.B., conceptualization, methodology, writing—review and editing; V.L., funding; P.Z., writing—review and editing; J.W., writing—review and editing; T.Y., writing—review and editing; M.H., writing—review and editing; G.Y., investigation; M.L. (Meng Liu), investigation; M.L. (Mengjia Li), investigation. All authors have read and agreed to the published version of the manuscript.

Funding: This research was funded by the Zhejiang Provincial Natural Science Foundation of China under grant No. LQ22E010007 and No. LTZ20E020001, the National Natural Science Foundation of China under grant No. 52001175 and the Science and Technology Bureau Project of Taizhou under grant No. 21gyb34 and the open fund of Zhejiang Provincial Key Laboratory for Cutting Tools under grant No. ZD202103.

Institutional Review Board Statement: Not applicable.

Informed Consent Statement: Not applicable.

Data Availability Statement: The data are not publicly available due to privacy.

Conflicts of Interest: The authors declare no conflict of interest.

References

1. Polmear, I.J.; Couper, M.J. Design and development of an experimental wrought aluminum alloy for use at elevated temperatures. *Metall. Trans. A* **1988**, *19*, 1027–1035. [CrossRef]
2. Oguocha, I.N.A.; Yannacopoulos, S. Precipitation and dissolution kinetics in Al-Cu-Mg-Fe-Ni alloy 2618 and Al-alumina particle metal matrix composite. *Mater. Sci. Eng. A* **1997**, *231*, 25–33. [CrossRef]
3. Polmear, I.; Pons, G.; Barbaux, Y.; Octor, H.; Sanchez, C.; Morton, A.; Borbidge, W.; Rogers, S.A. After Concorde: Evaluation of creep resistant Al-Cu-Mg-Ag alloys. *J. Mater. Sci. Technol.* **1999**, *15*, 861–868. [CrossRef]
4. Hutchinson, C.R.; Fan, X.; Pennycook, S.J.; Shiflet, G.J. On the origin of the high coarsening resistance of Ω plates in Al-Cu-Mg-Ag alloys. *Acta Mater.* **2001**, *49*, 2827–2841. [CrossRef]
5. Muddle, B.; Polmear, I. The precipitate Ω phase in Al-Cu-Mg-Ag alloys. *Acta Met.* **1989**, *37*, 777–789. [CrossRef]
6. Ringer, S.P.; Hono, K.; Polmear, I.J.; Sakurai, T. Nucleation of precipitates in aged Al-Cu-Mg-(Ag) alloys with high Cu:Mg ratios. *Acta Mater.* **1996**, *44*, 1883–1898. [CrossRef]
7. Knowles, K.M.; Stobbs, W.M. The structure of {111} age-hardening precipitates in Al-Cu-Mg-Ag alloys. *Acta Crystallogr. Sect. B Struct. Sci.* **1988**, *44*, 207–227. [CrossRef]
8. Ringer, S.P.; Yeung, W.; Muddle, B.C.; Polmear, I.J. Precipitate stability in Al-Cu-Mg-Ag alloys aged at high temperatures. *Acta Metall. Mater.* **1994**, *42*, 1715–1725. [CrossRef]
9. Bai, S.; Ying, P.; Liu, Z.; Wang, J.; Li, J. Quantitative transmission electron microscopy and atom probe tomography study of Ag-dependent precipitation of Ω phase in Al-Cu-Mg alloys. *Mater. Sci. Eng. A* **2017**, *687*, 8–16. [CrossRef]
10. Hono, K.; Sano, N.; Babu, S.S.; Okano, R.; Sakurai, T. Atom probe study of the precipitation process in Al-Cu-Mg-Ag alloys. *Acta Metall. Mater.* **1993**, *41*, 829–838. [CrossRef]
11. Zhou, X.; Liu, Z.; Bai, S.; Liu, M.; Ying, P. The influence of various Ag additions on the nucleation and thermal stability of Ω phase in Al-Cu-Mg alloys. *Mater. Sci. Eng. A* **2013**, *564*, 186–191. [CrossRef]
12. Zhou, Y.; Liu, Z.; Bai, S.; Ying, P.; Lin, L. Effect of Ag additions on the lengthening rate of Ω plates and formation of σ phase in Al-Cu-Mg alloys during thermal exposure. *Mater. Charact.* **2017**, *123*, 1–8. [CrossRef]
13. Bai, S.; Zhou, X.; Liu, Z.; Xia, P.; Liu, M.; Zeng, S. Effects of Ag variations on the microstructures and mechanical properties of Al-Cu-Mg alloys at elevated temperatures. *Mater. Sci. Eng. A* **2014**, *611*, 69–76. [CrossRef]
14. Bai, S.; Liu, Z.; Zhou, X.; Xia, P.; Liu, M. Stress-induced thickening of Ω phase in Al-Cu-Mg alloys containing various Ag additions. *Mater. Sci. Eng. A* **2014**, *589*, 89–96. [CrossRef]
15. Bakavos, D.; Prangnell, P.; Bes, B.; Eberl, F. The effect of silver on microstructural evolution in two 2xxx series Al-alloys with a high Cu:Mg ratio during ageing to a T8 temper. *Mater. Sci. Eng. A* **2008**, *491*, 214–223. [CrossRef]
16. Ringer, S.; Muddle, B.C.; Polmear, I.J. Effects of cold work on precipitation in Al-Cu-Mg-(Ag) and Al-Cu-Li-(Mg-Ag) alloys. *Metall. Mater. Trans. A* **1995**, *26*, 1659–1671. [CrossRef]
17. Li, Q.; Shenoy, R.N. DSC and TEM characterizations of thermal stability of an Al-Cu-Mg-Ag alloy. *J. Mater. Sci.* **1997**, *32*, 3401–3406. [CrossRef]
18. Chen, Y.-T.; Lee, S.-L.; Bor, H.-Y.; Lin, J.-C. Effect of natural aging and cold working on microstructures and mechanical properties of Al-4.6Cu-0.5Mg-0.5Ag alloy. *Metall. Mater. Trans. A* **2013**, *44*, 2831–2838. [CrossRef]
19. Bai, S.; Liu, Z.; Ying, P.; Wang, J.; Wang, A. Quantitative study of the solute clustering and precipitation in a prestretched Al-Cu-Mg-Ag alloy. *J. Alloys Compd.* **2017**, *725*, 1288–1296. [CrossRef]
20. Bai, S.; Yi, X.; Liu, Z.; Wang, J.; Zhao, J.; Ying, P. The influence of preaging on the strength and precipitation behavior of a deformed Al-Cu-Mg-Ag alloy. *J. Alloys Compd.* **2018**, *764*, 62–72. [CrossRef]

21. Lumley, R.N.; Polmear, I.J.; Morton, A.J. Interrupted aging and secondary precipitation in aluminum alloys. *Mater. Sci. Technol.* **2003**, *19*, 1483–1490. [CrossRef]
22. Li, Y.; Liu, Z.; Bai, S.; Zhou, X.; Wang, H.; Zeng, S. Enhanced mechanical properties in an Al-Cu-Mg-Ag alloy by duplex aging. *Mater. Sci. Eng. A* **2011**, *528*, 8060–8064. [CrossRef]
23. Vural, M.; Caro, J. Experimental analysis and constitutive modeling for the newly developed 2139-T8 alloy. *Mater. Sci. Eng. A* **2009**, *520*, 56–65. [CrossRef]
24. Ünlü, N.; Gable, B.M.; Shiflet, G.J.; Starke, E.A. The effect of cold work on the precipitation of Ω and θ′ in a ternary Al-Cu-Mg alloy. *Metall. Mater. Trans. A* **2003**, *34*, 2757–2769. [CrossRef]
25. Liu, X.-Y.; Wang, Z.-P.; Li, Q.-S.; Zhang, X.-L.; Cui, H.-X. Effects of pre-deformation on microstructure and properties of Al-Cu-Mg-Ag heat-resistant alloy. *J. Cent. South Univ.* **2017**, *24*, 1027–1033. [CrossRef]
26. Gazizov, M.; Kaibyshev, R. Effect of over-aging on the microstructural evolution in an Al-Cu-Mg-Ag alloy during ECAP at 300 C. *J. Alloys Compd.* **2012**, *527*, 163–175. [CrossRef]
27. Gazizov, M.; Kaibyshev, R. The precipitation behavior of an Al-Cu-Mg-Ag alloy under ECAP. *Mater. Sci. Eng. A* **2013**, *588*, 65–75. [CrossRef]
28. Gazizov, M.; Kaibyshev, R. Effect of pre-straining on the aging behavior and mechanical properties of an Al-Cu-Mg-Ag alloy. *Mater. Sci. Eng. A* **2015**, *625*, 119–130. [CrossRef]
29. Khalaj, G.; Khalaj, M.J.; Nazari, A. Microstructure and hot deformation behavior of AlMg6 alloy produced by equal-channel angular pressing. *Mater. Sci. Eng. A* **2012**, *542*, 15–20. [CrossRef]
30. Jandaghi, M.R.; Pouraliakbar, H.; Gharah Shiran, M.K.; Khalajd, G.; Shirazie, M. On the effect of non-isothermal annealing and multi-directional forging on the microstructural evolutions and correlated mechanical and electrical characteristics of hot-deformed Al-Mg alloy. *Mater. Sci. Eng. A* **2016**, *657*, 431–440. [CrossRef]
31. Cassada, W.A. Heterogeneous Precipitation in Al-Li-Cu Alloys. Ph.D. Dissertation, University of Virginia, Charlottesville, VA, USA, 1987.
32. Liu, M.; Klobes, B.; Maier, K. On the age-hardening of an Al-Zn-Mg-Cu alloy: A vacancy perspective. *Scr. Mater.* **2011**, *64*, 21–24. [CrossRef]
33. Marceau, R.K.; Sha, G.; Lumley, R.N.; Ringer, S.P. Evolution of solute clustering in Al-Cu-Mg alloys during secondary ageing. *Acta Mater.* **2010**, *58*, 1795–1805. [CrossRef]
34. Peng, J.; Bahl, S.; Shyam, A.; Haynes, J.A.; Shin, D. Solute-vacancy clustering in aluminum. *Acta Mater.* **2020**, *196*, 747–758. [CrossRef]
35. Zhu, A.W.; Starke, E.A., Jr. Strengthening effect of unshearable particles of finite size: A computer experimental study. *Acta Mater.* **1999**, *47*, 3263–3269. [CrossRef]
36. Nie, J.F.; Muddle, B.C. Microstructural design of high-strength aluminum alloys. *J. Phase Equilibria* **1998**, *19*, 543–551. [CrossRef]
37. Nie, J.F.; Muddle, B.C. Comments on the "dislocation interaction with semicoherent precipitates (Ω phase) in deformed Al-Cu-Mg-Ag alloy. *Scr. Mater.* **2000**, *42*, 409–413. [CrossRef]
38. Macchi, C.; Tolley, A.; Giovachini, R.; Polmear, I.; Somoza, A. Influence of a microalloying addition of Ag on the precipitation kinetics of an Al-Cu-Mg alloy with high Mg:Cu ratio. *Acta Mater.* **2015**, *98*, 275–287. [CrossRef]
39. Gazizov, M.R.; Boev, A.O.; Marioara, C.D.; Holmestad, R.; Aksyonov, D.A.; Gazizova, M.Y.; Kaibyshev, R.O. Precipitate/matrix incompatibilities related to the {111}Al Ω plates in an Al-Cu-Mg-Ag alloy. *Mater. Charact.* **2021**, *182*, 111586. [CrossRef]
40. Gazizov, M.; Boev, A.; Marioara, C.; Holmestad, R.; Gazizova, M.; Kaibyshev, R. Edge interfaces of the Ω plates in a peak-aged Al-Cu-Mg-Ag alloy. *Mater. Charact.* **2022**, *185*, 111747. [CrossRef]
41. Yang, S.; Zhao, X.; Chen, H.; Wilson, N.; Nie, J. Atomic structure and evolution of a precursor phase of Ω precipitate in an Al-Cu-Mg-Ag alloy. *Acta Mater.* **2022**, *225*, 117538. [CrossRef]